Role of the Flexible Loop of Hypoxanthine-Guanine-Xanthine Phosphoribosyltransferase from *Tritrichomonas foetus* in Enzyme Catalysis†

Narsimha Munagala, Vladimir J. Basus, and Ching C. Wang*

Department of Pharmaceutical Chemistry, University of California, San Francisco, California 94143-0446

Received November 27, 2000; Revised Manuscript Received January 31, 2001

ABSTRACT: The hypoxanthine-guanine-xanthine phosphoribosyltransferase (HGXPRTase), a type I PRTase, from *Tritrichomonas foetus*, is a potential target for antitritrichomonal chemotherapy. Structural data on all the type I PRTases reveal a highly flexible, 11−14-amino acid loop, presumably covering the active site. With the exception of a highly conserved Ser-Tyr dipeptide, the other amino acids constituting the loop vary widely among different PRTases. The roles of the conserved Ser73 and Tyr74 residues in the loop and the dynamics of the loop in *T. foetus* HGXPRTase were investigated using site-directed mutants, stop-flow kinetics, chemical modification, and two-dimensional $^{1}H-^{15}N$ heteronuclear NMR relaxation experiments. S73A, Y74F, and Y74E mutants of HGXPRTase exhibited a 5−7-fold increase in K_m for guanine and a 3−5-fold increase in K_m for PRPP compared to that of the wild type, reflecting the decreased affinity of binding for the two substrates. The k_{cat}'s for these mutant-catalyzed reactions, however, do not change appreciably from that of the wild-type enzyme. Stopped-flow fluorescence with a Y74W mutant showed no apparent quenching by adding either PRPP or GMP alone. When both PRPP and guanine were added together, however, the fluorescence was rapidly quenched, followed by a slow recovery as the enzyme-catalyzed reaction progressed, suggesting movement of the loop during catalysis. In the presence of 9-deazaguanine and PRPP, the rapidly quenched fluorescence was not recovered, suggesting a closed loop form. The accessibility of Trp74 in the flexible loop of the mutant enzyme was also analyzed using *N*-bromosuccinimide (NBS), which reacts specifically with the tryptophan residue. NBS reacted with the only tryptophan in the Y74W mutant enzyme and rendered the enzyme inactive. GMP or PRPP alone failed to protect the enzyme from NBS inactivation. However, the presence of both 9-deazaguanine and PPRP protected the enzyme, allowing it to retain up to 70% of its activity. An S75H mutant, labeled with [^{15}N]histidine, was used in the $^{1}H-^{15}N$ NMR study. Spectra obtained in the presence of enzyme substrates indicated an apparent stabilization of the loop only in the presence of 9-deazaguanine and PRPP. These experimental results thus clearly demonstrated stabilization of the flexible loop upon binding of both PRPP and guanine and suggested its involvement in enzyme catalysis.

Tritrichomonas foetus, an anaerobic flagellated protozoan, can cause embryonic death and infertility in cows (*1*, *2*). It lacks de novo purine nucleotide synthesis and relies primarily on its hypoxanthine-guanine-xanthine phosphoribosyltransferase (HGXPRTase)[1] for salvaging exogenous purine bases to replenish its purine nucleotide pool (*3*). This enzyme has been proven to be an excellent potential target in *T. foetus* for antitritrichomonial chemotherapy (*4*, *5*).

Purine phosphoribosyltransferases (PRTases) form a family of enzymes that catalyze transfer of the 5-phosphoribosyl moiety from D-α-5-phosphoribosyl-1-pyrophosphate (PRPP) to the imidazole N-9 of a purine base to form the corresponding purine nucleotide. Although there is little sequence homology among these enzymes, their crystal structures reported thus far suggest a common core of five parallel β-strands surrounded by three or four α-helices resembling a typical Rossmann dinucleotide binding fold among the type I PRTases (*3*−*8*). The only type II PRTase structure known thus far is of the quinolinic acid phosphoribosyltransferase (QAPRTase), which consists of an irregular α/β-barrel, with seven β-strands surrounded by six α-helices (*9*).

Another characteristic feature among the type I PRTase structures is a long flexible loop closely associated with the active site, often termed "the catalytic loop". In most of the previously determined structures of type I PRTase (*3*, *8*), the loop was usually highly disordered. With the effective use of nonreactive substrate analogues and transition state inhibitors, a few PRTase structures have been recently resolved with the stabilized loop covering the active site in a closed form (*4*, *5*, *7*). Among different type I PRTases, the loop generally consists of 11−14 amino acids with only a Ser-Tyr dipeptide in the loop highly conserved among them.

The type I purine PRTase-catalyzed reactions have been found to follow an ordered bi-bi mechanism, with binding of PRPP to the enzyme first, and then the binding of purine

† This work was supported by NIH Grant AI-19391.

* To whom correspondence should be addressed: Department of Pharmaceutical Chemistry, University of California, San Francisco, 513 Parnassus Ave., San Francisco, CA 94143-0446. Telephone: (415) 476-1321. Fax: (415) 476-3382. E-mail: ccwang@cgl.ucsf.edu.

[1] Abbreviations: HG(X)PRTase, hypoxanthine-guanine-(xanthine) phosphoribosyltransferase; PRPP, α-D-5-phosphoribosyl-1-pyrophosphate; GMP, guanosine monophosphate; PP_i, inorganic pyrophosphate; PRTase, phosphoribosyltransferase; NBS, *N*-bromosuccinimide; HSQC, heteronuclear single-quantum coherence; TSP, 3-(trimethylsilyl)propionic acid.

10.1021/bi0026932 CCC: $20.00
Published on Web 03/13/2001

base, followed by an ordered product release of PP_i and the nucleotide (*10*−*13*).

From the detailed kinetic data on isotope effects, Tao et al. (*14*) concluded that the orotate phosphoribosyltransferase (OPRTase)-catalyzed reaction appeared to follow an SN_1-type mechanism with the formation of a highly reactive and unstable oxocarbonium intermediate. The flexible loop could be responsible for protecting this reactive transition state at the active site of OPRTase as well as other type I PRTases (*15*). Subsequent studies, which showed ternary substrate complex structures of various PRTases, appeared to dispute the earlier notion of an SN_1 mechanism for the PRTase-catalyzed reactions. The crystal structure of *Trypanosoma cruzi* HGPRTase with a closed flexible loop at 1.8 Å resolution (*4*) was determined with 9-deaza-8-azahypoxanthine (HPP) and Mg^{2+}-PRPP bound to the enzyme. The presence of these two ligands should not be expected in a closed active site if the reaction was to follow an SN_1 mechanism. The human HGPRTase crystal structure with a transition state analogue Immucilin-GP and Mg^{2+}-pyrophosphate bound to the active site was recently determined (*16*), and showed also the presence of a highly ordered catalytic loop covering the active site. Most of the early crystal structures of type I PRTase determined with only a single ligand bound to the active site were, however, distinguished by a highly disordered catalytic loop, exemplified by the *T. foetus* HGXPRTase−GMP complex (*8*) and the human HGPRTase−GMP complex (*3*). From these crystal structures, it appears that the catalytic loop assumes a flexible open form. The closed loop structure of the *Tr. cruzi* HPRT clearly identifies extensive interaction between the conserved Tyr104 and bound PRPP (*4*). The aromatic ring of Tyr104 stacks over the PRPP molecule, with the hydroxyl group of the Tyr forming hydrogen bonds with the 5′-phosphate oxygen O3P. The structure of the human HGPRTase complexed with ImmGP and Mg^{2+}-PP_i showed the loop covering the active site, with the conserved Tyr104 forming a hydrogen bond with the 5′-phosphate of ImmGP (*16*).

The crystal structure of *T. foetus* HGXPRTase was previously determined at a resolution of 1.9 Å in an open form with the flexible loop between residues 73 and 83 invisible in the electron density map (*11*). Figure 1 describes a model based on the coordinates of the *T. foetus* HGXPRTase structure, with the flexible loop in its hypothetical open form. The modeled structure shows the loop in an open form. We describe here experiments aimed at illustrating the apparent role of this flexible loop in the catalytic process of the enzyme. Results from site-directed mutagenesis indicated the apparent importance of its highly conserved Ser73 and Tyr74 residues in substrate binding. A Trp residue introduced at position 74 which constituted the only Trp residue in the enzyme protein enabled a study on transient kinetics of the loop movement by stopped-flow fluorescence measurements. Substrate protection of Trp74 against the tryptophan-specific reagent *N*-bromosuccinimide (NBS) was also examined. An S75H mutant of the enzyme was analyzed with two-dimensional $^1H-^{15}N$ heteronuclear NMR spectroscopy. The dynamics of the loop with respect to the substrate binding observed in the spectra revealed stabilization of the loop in forming the PRPP−purine base−Mg^{2+} ternary complex at the active site of the enzyme and thus further suggested an SN_2 mechanism for the enzyme-catalyzed reaction.

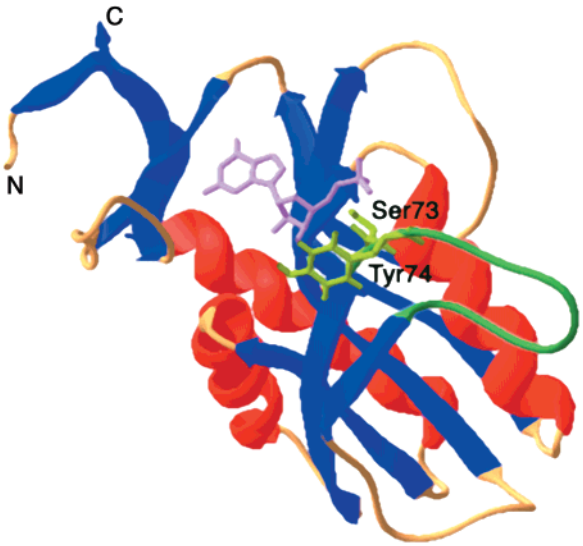

FIGURE 1: Structure of the HGXPRTase from *T. foetus*, with GMP (pink) bound in the active ste. The flexible loop (green) was modeled using Swiss-Model (*30*, *31*).

MATERIALS AND METHODS

Chemicals and Reagents. Hypoxanthine, guanine, xanthine, adenine, IMP, GMP, XMP, AMP, PP_i, PRPP, and NBS were all purchased from Sigma Chemical Co. (St. Louis, MO) and are of the highest purity available. 9-Deazaguanine was a generous gift from D. Borhani of the Southern Research Institute (Birmingham, AL).

Site-Directed Mutagenesis of the Cloned Gene Encoding T. foetus HGXPRTase. Oligonucleotide primers were designed and synthesized to generate various site-directed mutants of the encoding gene for *T. foetus* HGXPRTase cloned in the pBTfprt plasmid (*18*). Following polymerase chain reactions (PCRs) with the primers, each mutant DNA plasmid was transformed into an *Escherichia coli* mutant strain Sϕ606 (Δ*gpt-pro-lac, thi, hpt, Rec A*$^-$) (*17*), amplified, isolated, and sequenced for verification of the site-directed mutation.

Expression and Purification of the Recombinant Enzymes. *E. coli Sϕ*606 cells transformed with the pBTfprt expression plasmid were cultured, and expression of the recombinant enzyme was induced in the low-phosphate culture medium as previously described (*18*). The recombinant *T. foetus* HGXPRTase wild type and the site-directed mutants were each purified to homogeneity from the transformed cells as previously described (*18*), and stored at −70 °C without any detectable loss in activity for up to 6 months.

Recombinant *Giardia lamblia* GPRTase, cloned in a pBAce plasmid and expressed in transfected *E. coli* Sϕ606 cells, was purified to homogeneity as described previously (*19*).

Steady State Kinetic Study of the Enzyme-Catalyzed Reactions. The formation of GMP was followed spectrophotometrically at 245 nm using a Beckman DU-640 spectrophotometer equipped with a kinetics accessory as previously described (*10*). The assays were conducted in 100 mM Tris-HCl (pH 7.0) and 12 mM $MgCl_2$ at 37 °C. The extinction coefficient for formation of GMP from guanine under these conditions was 1770 M^{-1} cm^{-1}. Each K_m and V_{max} value was determined from multiple fixed substrate

concentrations and varying concentrations of the other substrate.

Analysis of the Kinetic Data. Data on the initial rates of the enzyme-catalyzed reaction were fitted to the equations for equilibrium ordered reactions (*20*), using the kinetics software from BioMetallics, Inc. (*k*cat), and IntelliKinetics (KinetAsyst) with Gauss−Newton analysis. The Lineweaver−Burk plots and the kinetic constants were obtained using the weighted linear regression.

Stopped-Flow Fluorescence Quenching. Transient kinetics of loop movement with respect to ligand binding were studied using a Y74W mutant of *T. foetus* HGXPRTase. Changes in the intrinsic fluorescence of tryptophan were monitored by measuring the fluorescence in a Hi-Tech KinetAsyst Double Mixing Stopped-Flow System. The excitation wavelength was 297 nm with a slit of 5 nm, and the emitted light was passed through a 320 nm cutoff filter. Ordinarily, five or six data sets were collected for each experiment and averaged.

Oxidation of the Tryptophan Residue with NBS. Chemical modification of the tryptophan residue with NBS in the Y74W mutant HGXPRTase was performed in 50 mM sodium acetate (pH 6.0) and 6 mM $MgCl_2$. Purified enzyme protein samples were titrated with various concentrations of NBS, and the residual enzyme activity and absorbance at 280 nm (A_{280}) were determined. The degree of tryptophan oxidation by NBS was calculated by the method described by Spande and Witkok (*21*).

$^1H-^{15}N$ Heteronuclear NMR Spectroscopy. Histidine was introduced into the flexible loop through site-directed mutagenesis. An S75H mutant was generated and purified from the transformed *E. coli* cells as described above. Backbone labeling of the histidine residues in the mutant enzyme was performed by growing the Sϕ606 cells, transformed with the mutant pBTfprt plasmid, in a modified low-phosphate induction medium (*18*). The modified medium contained MOPS salts supplemented with 0.2% glucose, 1.5 M thiamine, 20 mg/L adenine, and an equimolar mixture of Na_2HPO_4 and NaH_2PO_4 (0.1 mM) at pH 7.4. Instead of using Casamino acids, Thr, Phe, Leu, Ile, Lys, Val, Pro, and [α-^{15}N]histidine (Cambridge Isotope Laboratories) were each added to the medium at a concentration of 0.1 g/L. The labeled enzyme was isolated and purified from the cell lysate as described above. Samples for NMR spectroscopy, each having 0.24−0.3 mL of the enzyme solution, contained approximately 2 mM purified ^{15}N-labeled enzyme protein. Approximately 5% D_2O was added to the enzyme solution as a lock solvent. One-dimensional ^{15}N-edited NMR spectra were obtained on a Varian INOVA 600 instrument at 15 °C, whereas the two-dimensional spectra were obtained on a Bruker AVANCE 500 spectrometer equipped with a cryoprobe for extra sensitivity. Two-dimensional $^1H-^{15}N$ spectra were obtained with the gradient-enhanced HSQC sequence (*22*). One-dimensional ^{15}N-edited NMR spectra were obtained also with the HSQC sequence, with the evolution time set to zero. Typical acquisition times were ~16 h for the two-dimensional as well as one-dimensional spectra. A data set consisting of 2048 complex points in the direct dimension and 64 or 128 points in the nitrogen dimension was zero-filled to 256 points. ^{1}H chemical shifts relative to TSP were obtained using an external reference. ^{15}N chemical shifts were calculated indirectly on the basis of the proton reference (*23*).

Table 1: Kinetic Constants of Site-Directed Mutants of the Ser-Tyr Dipeptide in PRTases

	K_m (μM)		
	guanine	PRPP	k_{cat} (s^{-1})
HGXPRTase from *T. foetus*			
wild type	2.4 ± 0.7	46 ± 7.2	2.5 ± 0.2
S73A	11.2 ± 1.4	194.1 ± 20.2	2.3 ± 0.1
Y74F	14.5 ± 0.8	138.5 ± 15.6	1.8 ± 0.1
Y74E	16.4 ± 1.1	206.8 ± 22.3	1.5 ± 0.04
Y74W	4.3 ± 0.3	41.2 ± 5.2	3.1 ± 0.2
S75H	2.9 ± 0.1	28.7 ± 0.4	3.3 ± 0.1
GPRTase from *G. lamblia*			
wild type	16.4 ± 1.8	26.5 ± 2.2	76.7 ± 2.5
S96A	59.9 ± 8.5	136.8 ± 21.2	55.7 ± 4.2
Y97F	68.9 ± 4.2	172.3 ± 25.7	61.3 ± 4.8

RESULTS AND DISCUSSION

Role of Ser73 and Tyr74 in Substrate Binding. Sequence alignments among various purine PRTases in the flexible loop region show the presence of a highly conserved Ser-Tyr dipeptide (Figure 2). To evaluate its role in the catalytic reaction of *T. foetus* HGXPRTase, loop mutants at Ser73 and Try74 of the enzyme were prepared and their kinetic constants determined. As seen in Table 1, the S73A mutant enzyme-catalyzed reaction has a K_m of 11.2 ± 1.4 μM for guanine and 194.1 ± 20.2 μM for PRPP, which are 4−5-fold higher than that for the wild-type enzyme. The k_{cat} in the forward direction was 2.3 ± 0.1 s^{-1}, showing little change from the k_{cat} of 2.5 ± 0.2 s^{-1} for the wild-type reaction. The reactions catalyzed by mutants Y74F and Y74E have K_m's for guanine of 14.5 ± 0.8 and 16.4 ± 1.1 μM, respectively, whereas the K_m's for PRPP were determined to be 138.5 ± 15.6 and 206.8 ± 22.3 μM, respectively. There are, thus, in the two Tyr74 mutant-catalyzed reactions, a 6−7-fold increase in the K_m's for guanine and a 3−4-fold increase in the K_m's for PRPP over that of the wild-type enzyme. There are only minor variations in the k_{cat}'s for the forward reaction, as compared to that of the wild-type enzyme (Table 1). The Ser73-Tyr74 dipeptide is thus primarily involved in substrate binding to the active site in HGXPRTase and plays no apparent role in catalysis. This observation contrasts to that observed in the *Leishmania donovani* HGPRTase-catalyzed reaction (*15*), where it was shown that the conserved Ser and Tyr played a role in catalysis rather than substrate binding, and could be involved in protecting the carbonium ion transition state implied in an SN_1 reaction mechanism. Ser95 and Tyr96 mutants of the *L. donovani* HGPRTase showed negligible change from the wild type in the apparent K_m's for guanine, but had k_{cat}'s significantly decreased compared to that of the wild-type enzyme. There is no immediate explanation for the apparent discrepancy between the two findings. However, contrary to the above observation on *L. donovani* HGPRTase, a flexible loop S103R mutant (Munich variant) of the human HGPRTase, occurring as one of the several natural HPRTase deficient mutants in humans which lead to gout, showed an increase in K_m for hypoxanthine over that of the wild-type enzyme (*24*). In the crystal structure of *Tr. cruzi* HGPRTase (*4*), where the flexible loop is closed onto the active site, the conserved loop residue

```
                1                                  41                                  80
T.foetus                                                MTETPMMD DLERVLYNQD DIQKRIRELA AELTEFYEDK
B.subtitis                                                 MMKH DIEKVLISEE EIQKKVKELG AELTSEYQDT
T.cruzi                                                  MPREYE FAEKILFTEE EIRTRIMEVA KRIADDYKGK
T.gondii  MASKPIEDYG KGKGRIEPMY IPDNTFYNAD DFLVPPHCKP YIDKILLPGG LVKDRVEKLA YDIHRTYFG-
Human               MATRSPGVVI SDDEPGYDLD LFCIPNHYAE DLERVFIPHG LIMDRTERLA RDVMKEMGG-
G.lamblia             M ICSVTGKPVK DVLSTFFKDR NDVLESEVKK F--HLLATFE ECKALAADTA RRMNEYYKDV

                              101                                                 150
T.foetus  ------NPVM -ICVLTGAVF FYTDLLKHL- --DF------ ---QLEPDYI ICSSY-SGTK STGNLTISKD
B.subtitis ------FPLA -IGVLKGALP FMADLIKHI- --DT------ ---YLEMDFM DVSSYGNSTV SSGEVKIIKD
T.cruzi   GLRPYVNPLV LISVLKGSFM FTADLCRALS DFNV------ ---PVRMEFI CVSSYGEGVT SSGQVRMLLD
T.gondii  ------EELH IICILKGSRG FFNLLIDYLA TIQKYSGRES SVPPFFEHYV RLKSYQNDNS TGQLTVLS-D
Human     ------HHIV ALCVLKGGYK FFADLLDYIK ALNRNSDRSI ---PMTVDFI RLKSYCNDQS TGDIKVIGGD
G.lamblia A-----EPVT LVALLTGAYL YASLLTVHLT F--------- ---PYTLHFV KVSSY-KGTR QESVVFDEED

                              171                                                 200
T.foetus  LKTNIEGRHV LVVEDIIDTG LTMYQLLNNL QMRKPASLKV CTLCDKDIGK KAYDVPIDYC GFVVEN-RYI
B.subtitis LDTSVEGRDI LIIEDIIDSG LTLSYLVELF RYRKAKSIKI VTLLDKPSGR KA-DIKADFV GFEVPD-AFV
T.cruzi   TRHSIEGHHV LIVEDIVDTA LTLNYLYHMY FTRRPASLKT VVLLDKREGR RV-PFSADYV VANIPN-AFV
T.gondii  DLSIFRDKHV LIVEDIVDTG FTLTEFGERL KAVGPKSMRI ATLVEKRTDR SN-SLKGDFV GFSIED-VWI
Human     DLSTLTGKNV LIVEDIIDTG KTMQTLLSLV RQYNPKMVKV ASLLVKRTPR SV-GYKPDFV GFEIPD-KFV
G.lamblia LKQLKEKREV VLIDEYVDSG HTIFSIQEQI KHAKICSCFV KDVDAIKKHS ALADTKMFYG YTPMPKGSWL

                              221
T.foetus  IGYGFDFHNK YRNLPVIGIL KESVYT
B.subtitis VGYGLDYAER YRNLPYIGVL KPAVYES
T.cruzi   IGYGLDYDDT YRELRDIVVL RPEVYAEREA ARQKKQRAIG SADTDRDAKR EFHSKY
T.gondii  VGCCYDFNEM FRDFDHVAVL SDAARKKFEK
Human     VGYALDYNEY FRDLNHVCVI SETGKAKYKA
G.lamblia IGFGLDDNGL RRGWAHLFDI NLSESEVTEF RRRLTEHIKG LNINGVNRY
```

FIGURE 2: Alignment of protein sequences of *T. foetus* HGXPRTase, *Bacillus subtilis* HGPRTase, *Tr. cruzi* HGPRTase, *To. gondii* HGXPRTase, human HGPRTase, and *G. lamblia* GPRTase. The bar indicates the sequence of the flexible loop, with the conserved Ser-Tyr dipeptide.

Tyr104 interacts through its hydroxyl group with the PRPP 5′-phosphate, whereas the aromatic ring of Tyr104 is stacked on the ribose moiety of PRPP, suggesting that Tyr104 is directly involved with PRPP binding.

To further verify the role of the conserved loop dipeptide in purine PRTases, the corresponding mutants of *G. lamblia* GPRTase Ser96 and Tyr97 in the flexible loop (*18*) were generated and characterized. As shown in Table 1, the reaction catalyzed by the S96A mutant has a K_m of 59.9 ± 8.5 μM for guanine and 136.8 ± 21.2 μM for PRPP, which are 4−5-fold higher than that of the wild type, whereas the k_{cat} for the forward reaction remained largely unchanged. The Y97F mutant also exhibited 4- and 6-fold increases in the K_m's for guanine and PRPP, respectively (Table 1), over that of the wild type (*11*), whereas k_{cat} for the mutant-catalyzed forward reaction did not change appreciably from that of the wild-type enzyme. Therefore, we conclude that the role of the conserved Ser-Tyr dipeptide in the flexible loop is predominantly in binding the substrates, PRPP as well as the purine base, to the catalytic pocket of the enzyme.

Stopped-Flow Fluorescence Quenching. In the crystal structure of *T. foetus* HGXPRTase with bound GMP (*8*), the flexible loop appeared to be disordered, and residues from position 73 to 83 could not be modeled due to poor electron density. To determine the steps involved in stabilizing the flexible loop during enzyme catalysis, which could involve closing of the active site in *T. foetus* HGXPRTase upon substrate binding (*7*, *26*), we tagged the loop with a Trp residue which also constituted the only tryptophan residue in the mutant enzyme protein. Thus, by constructing the Y74W mutant, we also placed a fluorescent tag on residue 74, which was found to be involved in substrate binding to

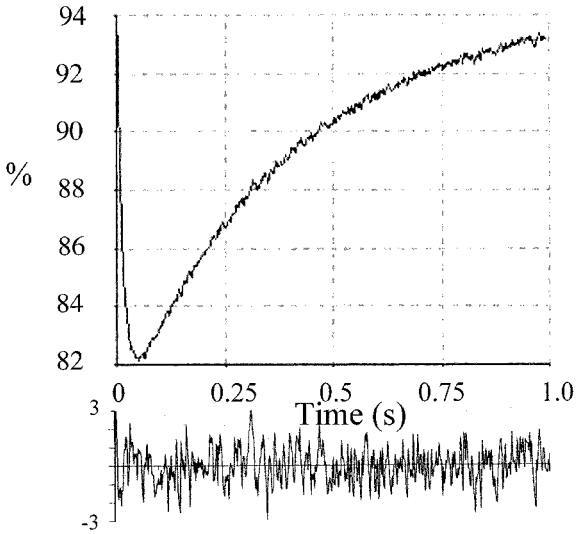

FIGURE 3: Rapid kinetics of Y74W HGXPRTase with PRPP and guanine. Stopped-flow fluorescence time course of the reaction with 2.5 μM Y74W enzyme protein mixed with 2 μM guanine and 500 μM PRPP in 100 mM Tris-HCl (pH 7.0) and 12 mM $MgCl_2$. The plot below the time course shows the residuals from the averaging of individual data sets.

the active site (see above). The reporter Trp at position 74 could be in a potentially heterogeneous environment during the catalytic process. Any environmental change or motion of the loop could be reflected in its intrinsic fluorescence. The Y74W mutant of HGXPRTase was first characterized kinetically by comparison with the wild-type enzyme. The K_m's for guanine and PRPP in the Y74W mutant-catalyzed reaction were determined to be 4.3 ± 0.3 and 41.2 ± 5.2 μM, respectively (Table 1). The k_{cat} for the forward reaction

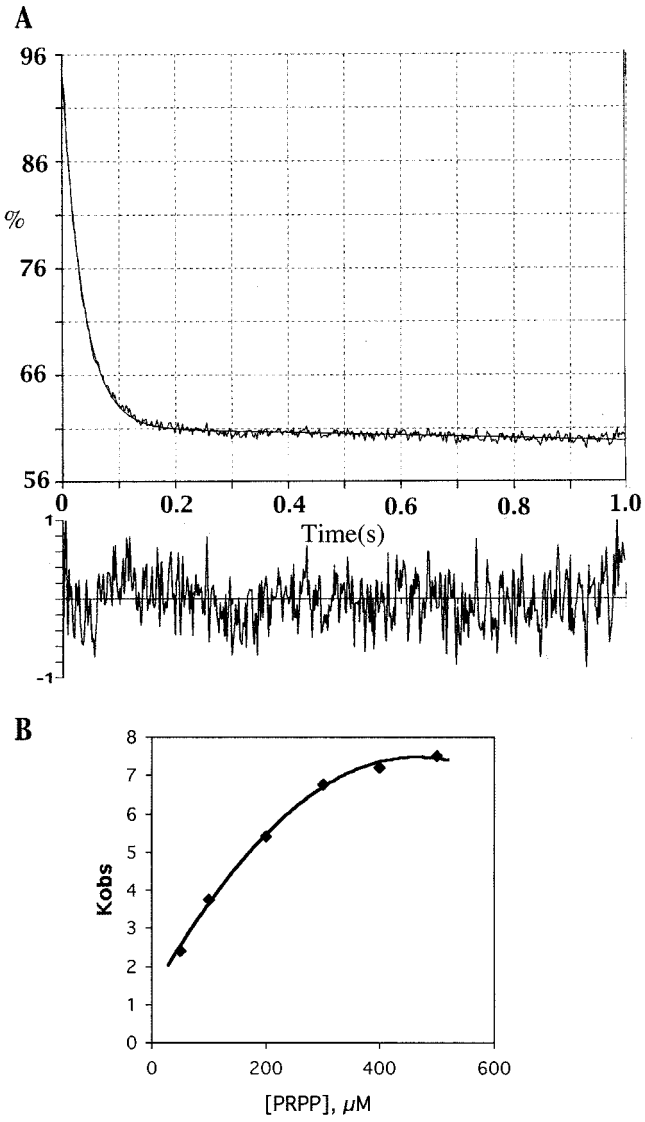

FIGURE 4: (A) Stopped-flow fluorescence kinetics of Y74W with 9-deazaguanine and PRPP. Fluorescence time course of 2.5 μM Y74W mixed with 200 μM 9-deazaguanine and 500 μM PRPP in 100 mM Tris-HCl (pH 7.0) and 12 mM $MgCl_2$. (B) Effect of PRPP concentration on the rate constants, k_{obs}, obtained from eq 1.

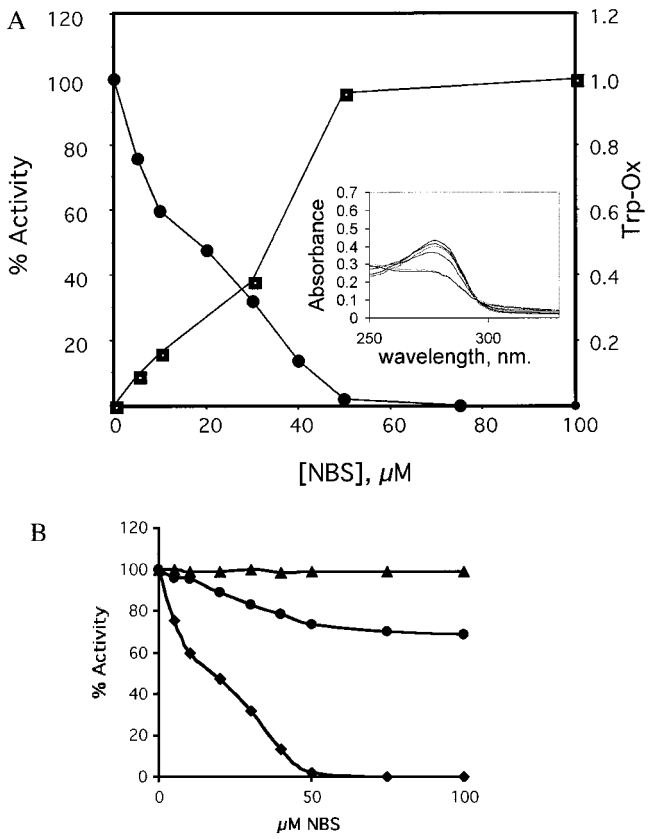

FIGURE 5: NBS oxidation of Trp74 in the flexible loop. (A) Effect of NBS modification on Y74W HGXXPRTase: (●) % GPRTase activity of Y74W and (■) degree of Trp oxidation, calculated as shown in Materials and Methods. The inset shows absorbance scans of the protein with NBS titration. (B) Effect of ligand binding on NBS oxidation of Y74W HGXPRTase: (◆) Y74W apoenzyme in the presence of NBS, (●) Y74W with 200 μM 9-deazaguanine and 1 mM PRPP in the presence of NBS, and (▲) wild-type HGXPRTase in the presence of NBS.

was 3.1 ± 0.2 s^{-1}, virtually indifferent from that of the wild type. Thus, the kinetic properties of the Y74W mutant are highly similar to that of the wild-type enzyme, and the mutant should be appropriate for the fluorescence quenching studies.

The rapid kinetics of ligand binding and the effect of ligand binding on the fluorescence of Trp74 present on the loop were studied using the rapid-mixing stopped-flow spectrofluorometer. The *T. foetus* HGXPRTase-catalyzed reaction, like those catalyzed by most other type I PRTases, follows an ordered bi-bi mechanism, in which PRPP binds first to the enzyme, followed by the binding of the purine base in the forward reaction (*9*). In the reverse reaction, it is GMP which binds first, followed by PP_i binding (*10*). When the free enzyme was mixed with 1 mM PRPP, there was no change in fluorescence. There was also no effect on the tryptophan fluorescence in the presence of 200 μM GMP (data not shown). The lack of any effect on the Trp74 fluorescence with either PRPP or GMP being bound to the enzyme could suggest an absence of any change in the environment of the loop tryptophan, which might suggest an open loop form of the enzyme in the presence of single substrates. This probability has been demonstrated previously in the crystal structure of the HGXPRTase−GMP complex (*8*), where the loop appeared to be flexible and most likely in an open form.

The combined effects of PRPP and guanine on the intrinsic flourescence of the Y74W mutant were monitored in transient phase kinetics, by mixing PRPP, guanine, and the enzyme in the observation cell. Figure 3 shows the time course of the change in Trp74 fluorescence during the catalytic process, wherein the fluorescence is first quenched rapidly and then regains its intensity at a much slower rate as the catalytic reaction progresses. This time course of fluorescence change could suggest loop movement during enzyme catalysis. The rapid fluorescence quenching in the beginning phase may indicate that the loop closes down onto the active site when both PRPP and guanine have been bound. Then, with the formation of products, the fluorescence regains its ground state, suggesting that the loop is back in its disordered open state again.

Nonreacting purine analogues have been used recently in determining the structures of PRTases. HPP (9-deaza-8-azahypoxanthine), together with PRPP, was used to determine the closed loop conformation of *Toxoplasma gondii* HGPRTase (*4*). Immucillin-GP, a transition state GMP analogue consisting of a 9-deazaguanine moiety, was used

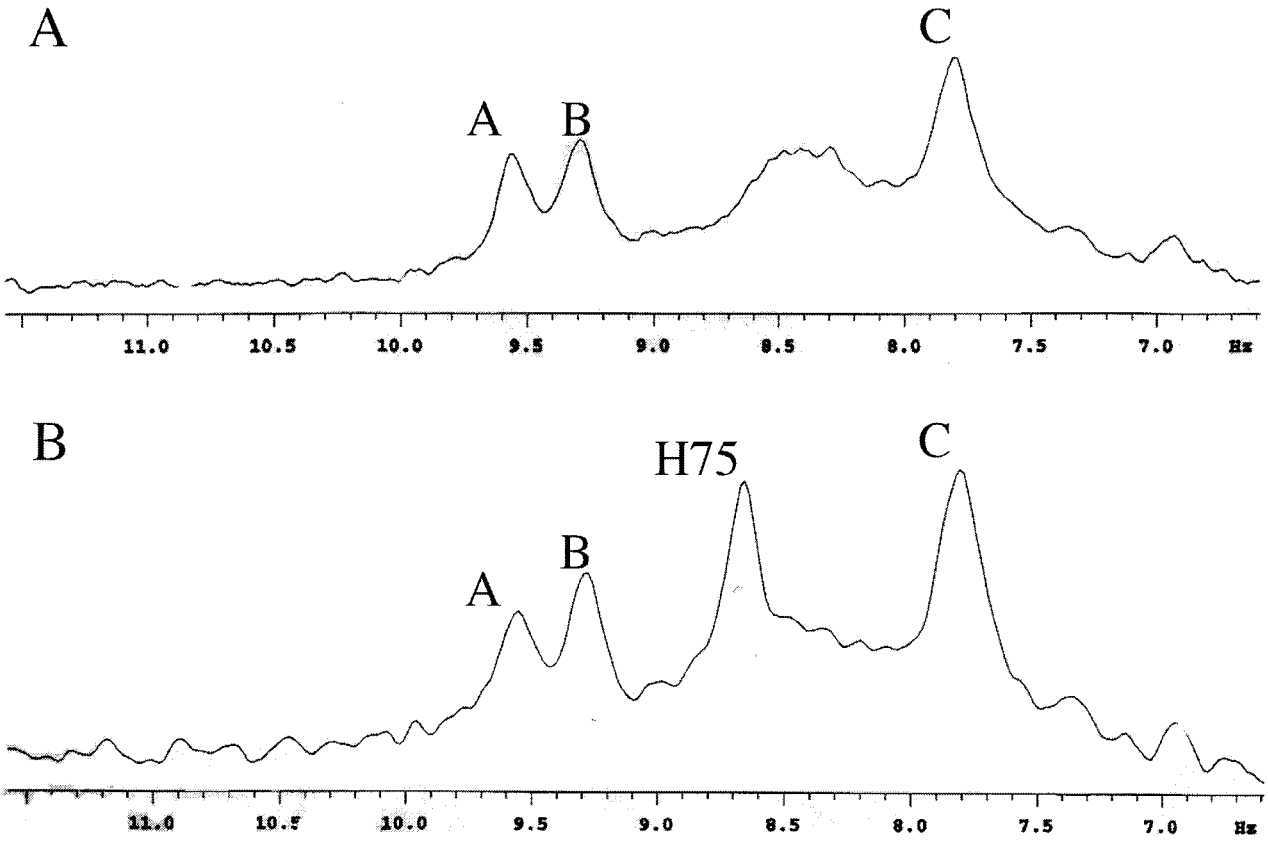

FIGURE 6: ^{1}H NMR spectra of wild-type HGXPRTase (A) and the S75H mutant (B). Histidine proton resonances were recorded with 2 mM enzyme protein in 0.1 M phosphate buffer (pH 7.0) and 0.1 M KCl.

to determine the crystal structures of *Plasmodium falciparum* HGXPRTase in the closed loop form (*5*) and *G. lamblia* GPRTase in its open loop form (*7*). To capture the enzyme−substrate complex in the active state in transient state kinetics, we replaced guanine with 9-deazaguanine in stopped-flow kinetic analysis. When the Y74W mutant enzyme was rapidly mixed with 500 μM PRPP and 200 μM 9-deazaguanine in the stopped-flow cell, the tryptophan fluorescence was rapidly quenched, and there was no apparent subsequent recovery as observed in the previous reaction with PRPP and guanine (Figure 4A). We therefore conclude that, when a nonreacting guanine analogue 9-deazaguanine was used along with PRPP, the flexible loop closes onto the active site and becomes stabilized. Due to the absence of any product formation or product release, the loop remains in its closed and fixed conformation (Figure 4A).

The transient phase kinetics of loop movement were further examined during the formation of the dead-end, closed enzyme complex with 9-deazaguanine and PRPP.

The fluorescence change in Figure 4A could fit best into a single-exponential equation of the form below, which includes both zero- and first-order reactions

$$F = \alpha_1 e^{-k_{obs}t} + C \qquad (1)$$

where t designates time and the pre-exponential term α_1 defines the amplitude of the reaction occurring with the rate k_{obs}. C is the offset for each data fit.

To investigate the effect of the PRPP concentration change on k_{obs}, the concentration of 9-deazaguanine was maintained at a constant level of 500 μM, and the PRPP concentration was varied between 50 and 500 μM. The results, presented in Figure 4B, indicate that k_{obs} varied with the PRPP concentration hyperbolically. It suggests a two-step mechanism of the loop movement toward closure of the active site. The first step is a binding step involving the formation of an initial equilibrium complex (E′−PRPP−9-deazaguanine) with an equilibrium dissociation constant K_i. This is followed by a slower rate k_i of the isomerization step to form the final closed form of the loop as shown in Scheme 1.

Scheme1

$$E + PRPP + 9DAG \overset{K_i}{\rightleftharpoons} E{\cdot}PRPP{\cdot}9DAG \overset{k_i}{\rightleftharpoons} E'{\cdot}PRPP{\cdot}9DAG$$

The open loop form of the enzyme is denoted as E and the final closed form as E′, whereas 9DAG designates 9-deazaguanine. The observed rate for the two-step reaction (k_{obs}) can be then defined by the following equation, assuming a steady state

$$k_{obs} = k_i[PRPP]/([PRPP] + K_i) \qquad (2)$$

Though the observed fluorescence change is due to the formation of a ternary complex of the enzyme with the two ligands, the above equation (eq 2) for a simple bimolecular reaction of the enzyme and PRPP is used to fit the data for k_{obs}, assuming the concentration of 9-deazaguanine is saturating. When the data for k_{obs} are fitted into the above equation, the estimated values for k_i and K_i were determined to be 9.9 s^{-1} and 63.3 μM, respectively. Since the steady state k_{cat} for the Y74W mutant-catalyzed forward reaction was estimated previously to be 3.1 s^{-1} (Table 1), whereas the rate for the loop closure is now determined to be 9.9 s^{-1}, the latter is

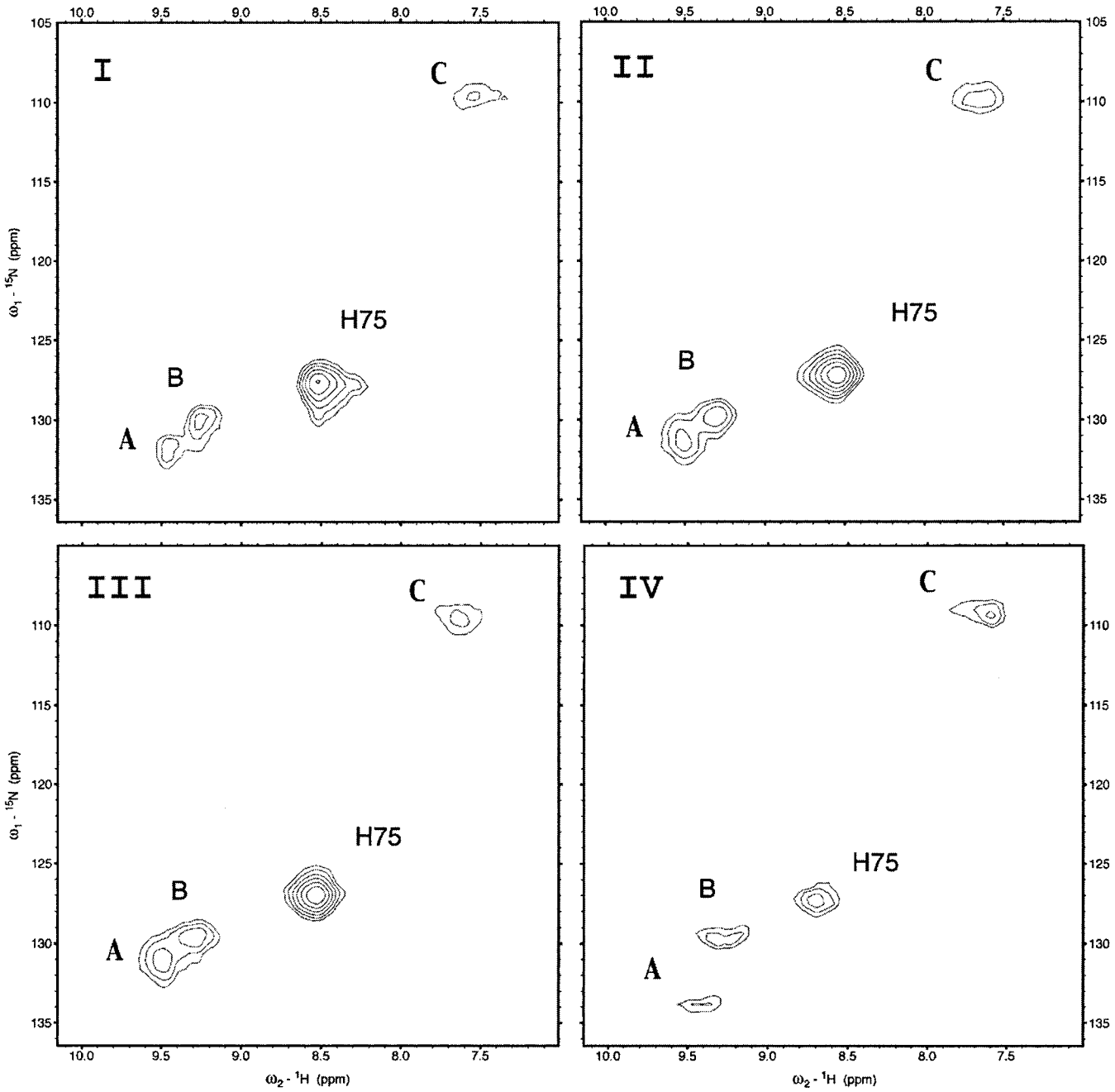

FIGURE 7: ^{1}H−^{15}N HSQC spectra at 4 °C of the S75H mutant of HGXPRTase: (I) 2 mM S75H enzyme, (II) 2 mM S75H enzyme and 200 μM GMP, (III) 2 mM S75H enzyme and 1 mM PRPP, and (IV) 2 mM S75H enzyme, 200 μM 9-deazaguanine, and 1 mM PRPP. Peaks labeled A−C are as in Table 2, and correspond to the native enzyme histidine residues, which were not assigned.

most unlikely the rate-limiting step in the HGXPRTase-catalyzed forward reaction. This conclusion agrees well with an earlier proposal that the rate of GMP release could be the rate-limiting step in PRTase enzyme-catalyzed reactions (*10*, *12*).

Chemical Modification of the Loop Trytophan. *N*-Bromosuccinimide (NBS) reacts specifically with tryptophan under conditions mentioned in Materials and Methods (*21*). It has been used extensively for probing tryptophan residues in proteins, and assaying their functions in the protein (*25*−*28*). The effect of NBS oxidation of the single tryptophan residue in the Y74W mutant of HGXPRTase was examined. Figure 5A shows that the enzymatic activity of the mutant decreases with increasing concentrations of NBS up to 50 μM when essentially all the activity is lost. Titration of the Y74W mutant protein with NBS indicated (Figure 5A) that the oxidation of 1 mol of Trp/mol of enzyme resulted in a total loss of enzyme activity.

Treatment of the wild-type enzyme, however, showed no detectable effect on enzymatic activity at all up to 100 μM NBS, suggesting that NBS oxidation of Trp74 in the flexible loop is the cause of inactivation of the mutant enzyme (Figure 5B). The effect of NBS oxidation of the Y74W mutant enzyme on its activity was also examined in the presence of substrates. The presence of either 1 mM PRPP or 200 μM GMP failed to protect the mutant enzyme from NBS inactivation, confirming the previous observation that binding of PRPP or GMP alone to the enzyme active site did not involve the flexible loop and Trp74 remained apparently accessible to NBS (data not shown). In the presence of 100

Table 2: Relative Intensities of the Resonances of the Histidine Residues in the $^1H-^{15}N$ HSQC Spectra at 4 °C

sample	resonance A	resonance B	resonance C	H75
free S75H	1.00	1.42	1.13	3.18
S75H with GMP	1.00	1.49	1.28	3.93
S75H with PRPP	1.00	1.56	1.48	4.49
S75H with PRPP and 9-deazaguanine	1.00	0.93	0.81	1.28

μM 9-deazaguanine and 1 mM PRPP, however, the mutant enzyme retained up to 70% of its activity upon treatment with 100 μM NBS (Figure 5B). These results concur with those observed with the stopped-flow fluorescence quenching experiments, wherein the loop appeared to remain flexible and open in the presence of PRPP or GMP, but was fixed and probably closed onto the active site when PRPP and 9-deazaguanine were both present.

Two-Dimensional $^1H-^{15}N$ Heteronuclear NMR Spectroscopy. To evaluate the mobility of the flexible loop in HGXPRTase using NMR spectroscopy, an S75H mutant was generated. The enzyme protein was specifically labeled with ^{15}N at the backbone nitrogen atoms of the histidine residues. Figure 6 shows the ^{15}N-edited proton NMR spectra of the wild-type HGXPRTase and the S75H mutant. The backbone amide proton resonances of the native histidines, His59, His97, and His165, were observed at approximately the same ^1H and ^{15}N chemical shifts in both proteins. But a new resonance at the proton and ^{15}N shifts of 8.50 and 128 ppm, respectively, were observed only in the S75H mutant sample (Figure 6). This new resonance can be attributed to the His75 residue in the mutant protein. The short T_2 ^1H and ^{15}N relaxation for the HGXPRTase with a dimer molecular mass of 47 kDa caused significantly reduced sensitivity of the HSQC spectra, due to decay of the signal during the required delays in the HSQC spectra. The His75 resonance at 4 °C in the free enzyme was clearly more intense than the resonances of the other three histidines as shown in Figure 7, due to longer ^1H and ^{15}N T_2 relaxation times for His75. Addition of either GMP or PRPP to the mutant enzyme showed no change in the HSQC spectra of His75. However, addition of both 9-deazaguanine and PRPP reduced considerably this resonance to an intensity similar to that of the other three histidine resonances. The relative intensities of the resonance at 4 °C, attributed to the four histidines, are listed in Table 2. The observed shift in the resonance of the unidentified peak C cannot be explained at the present time. Due to the long acquisition times required to observe these spectra (16 h each), and the low sensitivity of the resulting spectra, it was not possible to measure accurate relaxation times at this temperature. The HSQC intensities are, however, sensitive to the line widths of the ^1H and ^{15}N resonances as they approach the coupling constant between the amide−proton and the amide−^{15}N nucleus to which it is directly bonded (about 90 Hz coupling). These intensities are also sensitive to changes in coupling constants, which is expected to be the same for all amide protons in an isotropically rotating molecule. Thus, the observed higher intensity for the His75 resonance is most probably due to longer T_2 relaxation times, assuming isotropic tumbling, which indicates greater mobility of the backbone of the protein in this region. The apparent stabilization of the loop in the presence of 9-deazaguanine and PRPP would indicate a closed form of the loop in the enzyme−ligand complex.

Thus, in conclusion, by using various biochemical and biophysical methods for characterization of the dynamics of the flexible loop in HGXPRTase, we have been able to dissect the essential steps of the potential loop movement during the enzymatic reaction catalyzed by HGXPRTase. PRPP is presumed to bind first to the enzyme active site, as per the ordered bi-bi mechanism (*12*). This PRPP binding, which has no apparent effect on the conformation of the flexible loop, may induce a new enzyme−PRPP complex form with a modified active site wherein guanine can bind. We know now that this changed active site is not achieved by a closure of the flexible loop onto the active site. It could involve the movement of two other loops, the phosphate binding loop, often termed loop III, and the purine binding loop (loop IV). In *To. gondii* HGXPRTase, Heroux et al. (*29*) observed that loop III becomes ordered only when the enzyme binds to the ribose 5′-phosphate moiety of PRPP or GMP. The productive binding of guanine to the enzyme−PRPP complex could be achieved by an a priori movement of loops III and IV in the active site. Our present data suggest that the flexible loop then closes and becomes fixed on the active site thereafter so that the presumed SN_2 reaction could proceed between PRPP and the purine base in a closed chamber. On the other hand, it does not indicate whether PP_i thus formed in the reaction is released prior to or after opening of the flexible loop. Since GMP binding to the active site does not affect the loop in its flexible form, it is highly probable that the loop opening precedes GMP release. Release of the purine nucleotide was identified in kinetic studies as the rate-limiting step of the catalytic reaction in the forward direction (*9*, *11*). It could mean that the rate of loop opening could determine the overall rate of the forward reaction.

ACKNOWLEDGMENT

We thank Dr. Susan Miller of the University of California, San Francisco, for her helpful instructions in operating the stopped-flow fluorometer. Thanks are also due to Dr. David Borhani of the Southern Research Institute for his generous gift of 9-deazaguanine.

REFERENCES

1. Fitzgerald, P. R. (1986) *Veterinary Clinics of North America: Food Animal Practice 2*, 277−282.
2. Parsonson, I. M., Clark, B. L., and Dufty, J. (1974) *Aust. Vet. J. 50*, 421−423.
3. Eads, J. C., Scapin, G., Xu, Y., Grubmeyer, C., and Sacchettini, J. C. (1994) *Cell 78*, 325−334.
4. Focia, P. J., Craig, S. P., III, and Eakin, A. E. (1998) *Biochemistry 37*, 17120−17127.
5. Shi, W., Li, C. M., Tyler, P. C., Furneaux, R. H., Cahill, S. M., Girvin, M. E., Grubmeyer, C., Schramm, V. L., and Almo, S. C. (1999) *Biochemistry 38*, 9872−9880.
6. Schumacher, M. A., Carter, D., Ross, D. S., Ullman, B., and Brennan, R. G. (1996) *Nat. Struct. Biol. 3*, 881−887.
7. Shi, W., Munagala, N. R., Wang, C. C., Li, C. M., Tyler, P. C., Furneaux, R. H., Grubmeyer, C., Schramm, V. L., and Almo, S. C. (2000) *Biochemistry 39*, 6781−6790.
8. Somoza, J. R., Chin, M. S., Focia, P. J., Wang, C. C., and Fletterick, R. J. (1996) *Biochemistry 35*, 7032−7040.
9. Eads, J. C., Ozturk, D., Wexler, T. B., Grubmeyer, C., and Sacchettini, J. C. (1997) *Structure 5*, 47−58.
10. Munagala, N. R., Chin, M. S., and Wang, C. C. (1998) *Biochemistry 37*, 4045−4051.

11. Page, J. P., Munagala, N. R., and Wang, C. C. (1999) *Eur. J. Biochem. 259*, 565−571.
12. Xu, Y., Eads, J., Sacchettini, J. C., and Grubmeyer, C. (1997) *Biochemistry 36*, 3700−3712.
13. Yuan, L., Craig, S. P. d., McKerrow, J. H., and Wang, C. C. (1992) *Biochemistry 31*, 806−810.
14. Tao, W., Grubmeyer, C., and Blanchard, J. S. (1996) *Biochemistry 35*, 14−21.
15. Jardim, A., and Ullman, B. (1997) *J. Biol. Chem. 272*, 8967−8973.
16. Shi, W., Li, C. M., Tyler, P. C., Furneaux, R. H., Grubmeyer, C., Schramm, V. L., and Almo, S. C. (1999) *Nat. Struct. Biol. 6*, 588−593.
17. Chin, M. S., and Wang, C. C. (1994) *Mol. Biochem. Parasitol. 63*, 221−229.
18. Kanaani, J., Somoza, J. R., Maltby, D., and Wang, C. C. (1996) *Eur. J. Biochem. 239*, 764−772.
19. Sommer, J. M., Ma, H., and Wang, C. C. (1996) *Mol. Biochem. Parasitol. 78*, 185−193.
20. Cleland, W. W. (1963) *Biochim. Biophys. Acta 67*, 104−137.
21. Spande, T. F. W. (1967) *Methods Enzymol. 11*, 498−508.
22. Kay, L. E., Keifer, P., and Saarinen, T. (1992) *J. Am. Chem. Soc 114*, 10663−10665.
23. Wishart, D. S., and Sykes, B. D. (1994) *J. Biomol. NMR 4*, 171−180.
24. Wilson, J. M., Stout, J. T., Palella, T. D., Davidson, B. L., Kelley, W. N., and Caskey, C. T. (1986) *J. Clin. Invest. 77*, 188−195.
25. Beattie, B. K., Prentice, G. A., and Merrill, A. R. (1996) *Biochemistry 35*, 15134−15142.
26. Bray, M. R., Johnson, P. E., Gilkes, N. R., McIntosh, L. P., Kilburn, D. G., and Warren, R. A. (1996) *Protein Sci. 5*, 2311−2318.
27. Rao, M. N., Kembhavi, A. A., and Pant, A. (1996) *Biochem. J. 319*, 159−164.
28. Maras, B., Valiante, S., Orru, S., Simmaco, M., Barra, D., and Churchich, J. E. (1999) *J. Protein Chem. 18*, 259−268.
29. Heroux, A., White, E. L., Ross, L. J., and Borhani, D. W. (1999) *Biochemistry 38*, 14485−14494.
30. Guex, N., and Peitsch, M. C. (1997) *Electrophoresis 18*, 2714−2723.
31. Peitsch, M. C. (1996) *Biochem. Soc. Trans. 24*, 274−279.

BI0026932